RESEARCH PAPER

Fatigue performance of ultra-high-strength steel laser cut notches under variable amplitude loading

Kalle Lipiäinen[1] · Antti Ahola[1] · Timo Björk[1]

Abstract

Experimental fatigue tests with variable amplitude (VA) load were conducted for notched uncoated and hot-dip galvanized (HDG) notched laser cut components made of S960 ultra-high-strength steel (UHSS). Tests were conducted with low (constant minimum) and high (constant maximum) mean stresses and major differences between fatigue lives with the tests on identical equivalent stress were found. A multiparametric 4R method application, in conjunction with the theory of critical distances (TCD) to obtain fatigue-effective stresses at notch, was utilized on the mean stress correction and fatigue strength assessment. The introduced 4R method was proven to be highly efficient to consider different mean stress levels based on the experimental results and different loading and specimen types could be evaluated with single FAT class.

Keywords Laser cutting · Hot-dip galvanizing · Fatigue performance · Variable amplitude loading · Ultra-high-strength steel

1 Introduction

Cut edges on ultra-high-strength steel (UHSS) structures have been recently studied due to increased performance of welded joints when post-weld treatments (PWTs) are applied. Cut geometries are particularly interesting since stress concentration factors (SCFs) reduce fatigue life. A cut plate component of a truck fatigue performance was studied by Wang et al. [1]. Stress concentrations highlight local behavior which is a key in variable amplitude (VA) load fatigue strength assessment.

Lipiäinen et al. [2] introduced 3D-scanned surface quality–based 4R fatigue performance assessment application. However, the use of plain surface roughness in fatigue strength assessment is problematic. Figure 1 illustrates an example where specimens with high surface roughness with as-rolled surfaces machined have higher fatigue performance than specimen with practically smooth laser cut edge where

✉ Kalle Lipiäinen
kalle.lipiainen@lut.fi

1   Laboratory of Steel Structures, Lappeenranta-Lahti University of Technology LUT, P.O. Box 20, 53851 Lappeenranta, Finland

as-rolled surfaces were found critical in fatigue tests. Further studies with hot-dip galvanized (HDG) specimens introduced need for improved stress obtaining method due to liquid metal assisted cracking (LMAC) neglected the influence of surface quality. Moreover, fractography revealed brittle crack-like layer up to 25 μm which has significant influence on fatigue. Its influence together with surface quality is illustrated in Figs. 4 and 5 as fatigue test data and SEM (scanning electron microscope) fractography.

Theory of critical distances (TCD) described in [3] has been applied in fatigue strength assessment, e.g., in [4–6]. The authors [7] introduced and applied TCD method–based stress obtaining for multiparametric 4R fatigue strength assessment model. This study focuses on the fatigue performance as the laser cutting and hot-dip galvanizing are already discussed in [7, 8]. For the case presented in Fig. 1, the TCD method has better estimation of fatigue performance due to critical distance with 25-μm crack modelled on surface quality valleys which decreases the effect of external surface roughness in a similar way than in experimental tests.

Palmgren–Miner rule is typically used with VA loads (Eq. (1)). Damage sum (D) is 0.5 according to IIW recommendations [9] and BS7608 [10]. Damage sum is recommended to be reduced (up to $D = 0.2$) if stress ratio varies. Schijve [11] provides guidelines for conducting fatigue testing and assessing fatigue life with VA load.
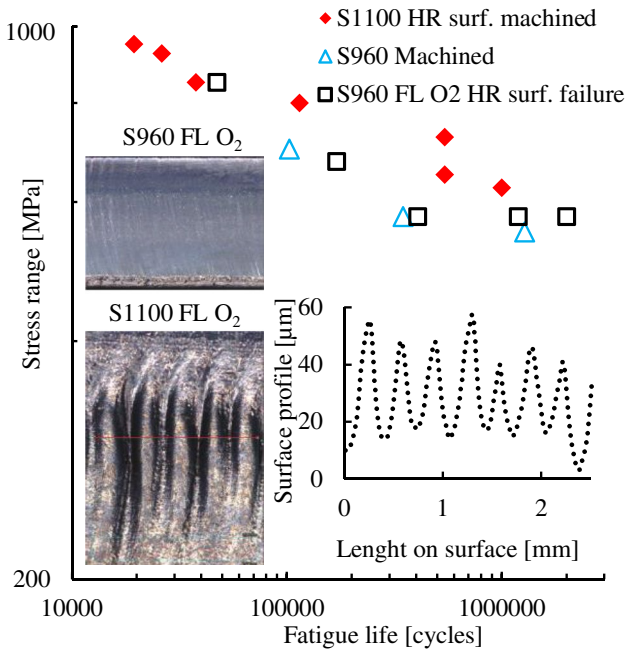
Fig. 1 Demonstration of problematic use of surface quality in fatigue performance assessment

$$D = \sum_{i}^{n} \frac{n_i}{N_i} \qquad (1)$$

Fatigue tests are most typically conducted with stress ratio $R = 0.1$. In this study, fatigue tests are conducted with variable amplitude (VA) block-type loading. Fatigue-loaded structures are subjected to VA load in many cases. Performance of

the product could be improved by accurate tools to assess VA load in design phase. High-accuracy fatigue strength assessment methods could motivate load spectrum estimation as the load becomes highest source of uncertainty.

Recently, VA load–controlled fatigue tests have been performed; Shams-Hakimi et al. [12] tested welded and HFMI-treated S460 specimens in high-cycle regime and found mean stress important parameter for fatigue performance as the high mean stress resulted significantly reduced fatigue performance. Leitner et al. [13] tested high-strength HFMI-treated welds without mean stress ($R = -1$) and low mean stress levels and found damage parameter $D = 1.0$ conservative in some cases. Liu et al. [14] studied the effect of mean stress with welded joint (in as-welded condition) and found decreasing minimum stress to increase fatigue life and damage sums up to $D = 1.5$.

TCD-based 4R method application where mean stress correction is considered via local cyclic behavior was evaluated in this study. For background information of used method, Fig. 2 provides some points on fatigue behavior. With fractography, correlation between initial cracks and surface quality can be evaluated. The effect of peak-loading is important when considering influence of small cycles on accumulated fatigue damage.

2 Fatigue strength assessment of VA loads in the 4R method

Rainflow analyses with Palmgren–Miner linear damage (Eq. (1)) is used to evaluate VA load with FAT classes intended for constant amplitude (CA) loads (Eq. (2)). A
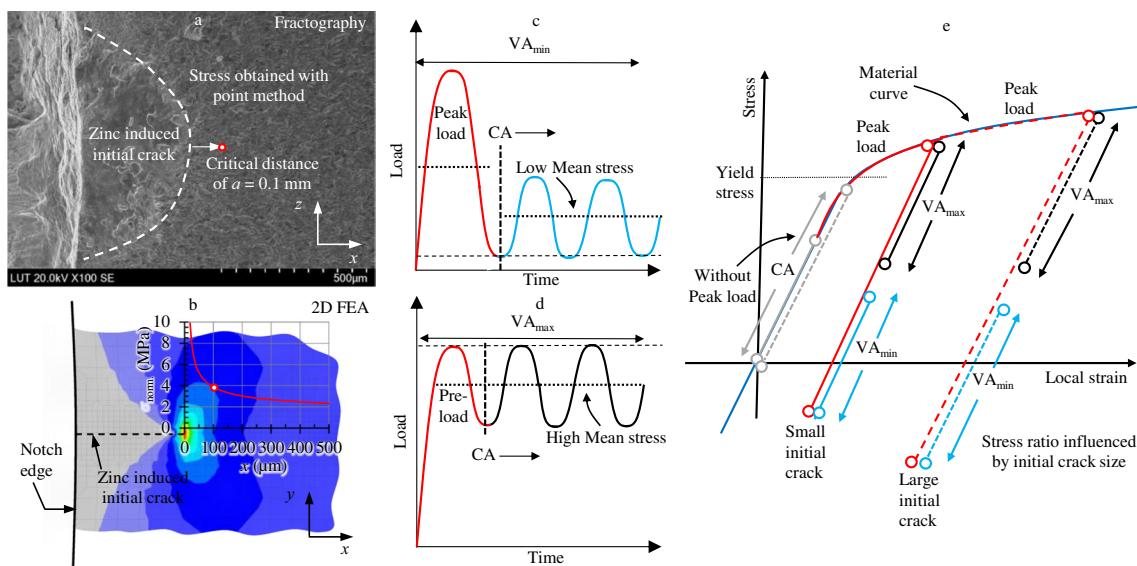

Fig. 2 4R TCD method background information

modified rainflow method was used successfully for multi-axial fatigue case by Bibbo et al. [15]. Damage parameter D is used to adjust safety factor and fatigue performance variations. A use of $D = 0.5$ and $D = 0.2$ results in stress factors of 1.25 and 1.7 (with the slope parameter $m = 3$), respectively. Nykänen et al. [16] used a parametric method, namely the 3R method at the time of the publication for assessing the fatigue strength of welded joints under variable amplitude loading. The analysis procedure of the 4R method for CA loads is thoroughly presented in [7]. To be used with VA loads, the local behavior at the notched component should be estimated for each cycle and then combined with the equivalent stress concept with the Smith–Watson–Topper (SWT) mean stress correction as follows:

$$\Delta\sigma_{k,ref,eq.} = \sqrt[m_{ref}]{\frac{1}{D}\frac{\sum i^{n_i}\left(\frac{\Delta\sigma_{k,i}}{\sqrt{1-R_{local,i}}}\right)^{m_{ref}}}{\sum i^{n_i}}} \tag{2}$$

where $\Delta\sigma_{k,ref,eq.}$ is the equivalent mean stress corrected stress range, n is the number of cycles (at each block), $\Delta\sigma_k$ is the (linear-elastic) effective stress range obtained by the TCD method, and R_{local} is the local stress ratio (see also further equations for an explanation about the 4R method). Linear-elastic notch stresses, as per the TCD method, are applied in the analysis, but the elastic–plastic behavior is analytically obtained using the Neuber's notch rule. The (maximum) linear-elastic fatigue-effective stress (as per the TCD method) is obtained as follows:

$$\sigma_k = K_f(a_{tcd})\sigma_{nom,max} \tag{3}$$

where $K_f(a_{tcd})$ is the (linear-elastic) effective notch stress concentration factor (SCF) obtained at the distance of a_{tcd}, a_{tcd} is the critical distance in the point method (PM), and $\sigma_{nom,max}$ is the maximum nominal stress of external loading. The elastic–plastic behavior at the notch is described with the Ramberg–Osgood (R-O) material models, considering the monotonic and cyclic behavior as follows:

$$\varepsilon = \frac{\sigma}{E} + \left(\frac{\sigma}{H}\right)^{\frac{1}{n}} \tag{4}$$

$$\Delta\varepsilon = \frac{\Delta\sigma}{E} + \left(\frac{\Delta\sigma}{2H}\right)^{\frac{1}{n}} \tag{5}$$

where σ and ε are the true stress and true strain values, E is the modulus of elasticity, H is the strength coefficient, and n is the strain hardening exponent. In the S960 UHSS grade with rather high yield strength to ultimate strength ratio, the following parameters can be approximated: $H = 1.3f_u$ and $n = 0.03$ [2, 17]. The linear-elastic notch stress can be converted to the elastic–plastic behavior at the notch root with Neuber's rule. In this evaluation, the residual stress state

resulting from the plate edge cutting can be considered. For the monotonic load (first cycle with the highest load), Neuber's rule can be written as follows:

$$\varepsilon = \frac{(\sigma_k + \sigma_{res})^2}{\sigma E} \tag{6}$$

where σ_{res} is the residual stress. For the cyclic loads, Neuber's rule can be written as:

$$\Delta\varepsilon_i = \frac{\Delta\sigma_{k,i}^2}{\Delta\sigma_i E} \tag{7}$$

where the Δ-values represent the corresponding range values. Under VA loading, the relaxation of the stress is considered, i.e., the stress from the previous cycle is regarded as a starting point for the next cycle. In the experiments of this study, the highest VA load cycle is at the start of the loading block and consequently, the equations for the cyclic curves (Eqs. (5) and (7)) are applied for the cycles after the first cycle (see also Section 3.2 for further details of the experimental campaign). Figure 2 schematically illustrates the relaxation of residual stress and shows the differences in the local behavior under low and high mean stress level. In addition, the local stresses and degree of plasticization are higher for the HDG components due to the larger initial crack depth and thus higher effective SCF in the TCD method. For each individual cycle, the local stress ratio is obtained as follows:

$$R_{local,i} = \frac{\sigma_{min,i}}{\sigma_{max,i}} \tag{8}$$

where σ_{min} and σ_{max} are the minimum and maximum local stress (see Fig. 2) for cycle i. The mean stress–corrected reference stress range for each cycle i can be written as (see also Eq. (2)):

$$R_{k,ref,i} = \frac{\Delta\sigma_{k,i}}{\sqrt{1-R_{local,i}}} \tag{9}$$

The parametric procedure and 4R method principle are schematically explained in Fig. 2. The TCD-based 4R method application benefits from a possibility to be drawn graphically enabling easier adaption to new applications and understanding the principle of the method. Figure 2a and 2b show fractography obtained initial crack and corresponding FEA with a normalized stress ($\sigma_{norm.}$) distribution from which the fatigue-effective stress can be obtained as per the TCD (PM) method. A basic case of high peak load (Fig. 2c) and pre-load (Fig. 2d) followed by a constant amplitude load is schematically plotted in Fig. 2e. In this study, residual stresses are not considered, and first cycle begins from the origin ($\sigma_{res} = 0$). However, residual stresses can be used to

modify start point of first cycle and implementing residual stresses will be studied in future work.

The introduced model is deterministic (with an exception of the statistically determined master curve), whereas, e.g., machine learning– and artificial intelligence–based methods can be found beneficial, but they can include so-called black boxes and are typically based on probabilistic approach.

3 Experimental methods

3.1 Specimens

A direct-quenched low-alloyed UHSS steel grade with 960 MPa yield strength was used for specimens. A total number of 20 fatigue tests were conducted (10 VA_{min} and 10 VA_{max}). The specimen geometries, preparation, and test arrangement are illustrated in Fig. 3. Further information on the test specimens can be found from [2, 7] in which CA loads were studied with identical specimens. Laser cut specimens in the uncoated and hot-dip galvanized conditions were used to experimentally evaluate the influence on VA loading on the fatigue performance. In respect to net cross-section, the SCFs varied from 1.84 to 2.48. HDG incudes crack-like defects via hydrogen embrittlement (HE) and liquid metal embattlement (LME) or liquid metal assisted cracking (LMAC). Moreover, on notched components laser cutting incudes up to 25-µm brittle layer where intergranular crack propagation occurs. The effect of initial crack length is included in analysis in Section 5.

3.2 Variable amplitude loading

A VA block with 7244 cycles was constructed and used as a sinusoidal wave signal for servo-hydraulic fatigue test machine (a capacity of 150 kN). The test frequency was set as per the magnitude of loading and was ≈1 Hz. Two different VA loading configurations were used: (1) constant minimum (VA1–3, Table 1) and (2) constant maximum (VA4–6) load to investigate the effect of mean stress on the fatigue strength capacity.

The load block was constructed to include one peak load and increasing number of smaller cycles. The spectrum load was constructed by following guidance presented by Köhler et al. [18]:

$$H_i = H_e exp \left\{ -1nH_0 \left(\frac{\Delta\sigma_{nom,i}}{\Delta\sigma_{nom,max}} \right)^v \right\} \tag{10}$$

where H_0 is the block length ($H_0 = 1000$ cycles was chosen in this case), $\Delta\sigma_{nom,i}$ is the nominal stress range of individual cycle, and $\Delta\sigma_{nom,max}$ is the maximum nominal stress range of the spectrum ($\Delta\sigma_{nom,max}$ is equal to 625 MPa, 550 MPa, 475 MPa, and 400 MPa, see Table 1). The Gaussian shape factor of the spectrum of $v = 2.0$ was chosen for the study as a representative value for random spectrum loads. In addition, to avoid resulting minor cycles in the block loading with the concern of being under the fatigue limit, the spectrum was scaled with the factor of $p = 0.4$. This corresponds to a case in which the lowest stress range equals to 40% of the highest stress range. The scaled stress range for each cycle can be obtained as follows:

$$\Delta\sigma_{nom,i,p} = \left\{ \frac{\Delta\sigma_{nom,i}}{\Delta\sigma_{nom,max}} (1-p) + p \right\} \Delta\sigma_{nom,i} \tag{11}$$

The loading was discretized into 21 different sequences (from $\Delta\sigma_{nom,i}/\Delta\sigma_{nom,max} = 1.0$ to 0, with a 0.05 step size). Scaling factor of 0.4 ($\sigma_{min}/\sigma_{max}$) was used to construct VA loads like demonstrated in Table 1. VA load with IDs are listed in Table 1 and shown with maximum stress and equivalent rainflow method obtained stress. The IDs are used in Table 5 in the Appendix with fatigue
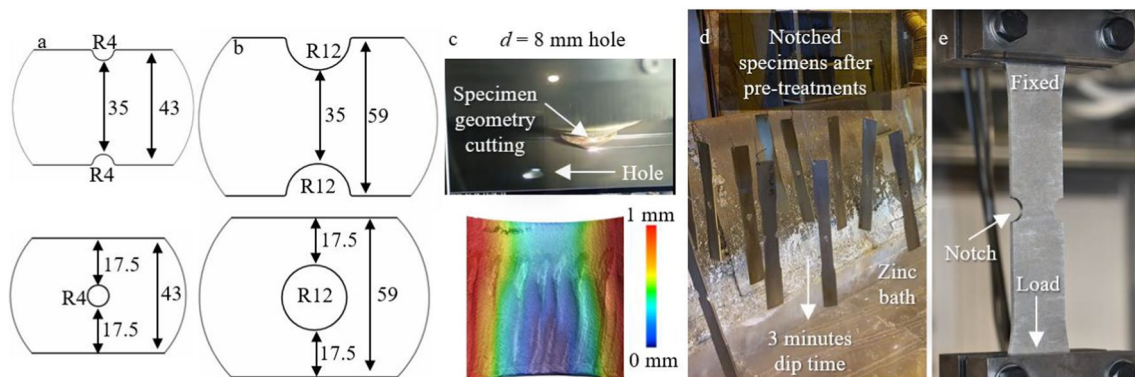

Fig. 3 Notch geometries for the (**a**) $d = 8$ mm and (**b**) $d = 24$ mm notch geometries, (**c**) cutting $d = 8$ mm hole specimen and surface quality, (**d**) galvanizing notched specimens, and (**e**) test arrangement

Table 1 Load spectrums and example of VA1 stress and load sequency. The applied stress ranges refer to stress at the net cross-section ($b = 35$ mm, $t = 6$ mm, see Fig. 3)

Load ID	Constant level	$\Delta\sigma_{nom,max}$ [MPa]	$\Delta\sigma_{nom,min}$[a] [MPa]	$\Delta\sigma_{eq.}$ ($m = 3$) [MPa]	Mean stress type (Local stress)	Scaling Factor	n
VA1	Min	625	250	337		1	1
						0.97	2
						0.94	4
					Low	0.91	7
VA2	Min	550	220	297	mean	0.88	12
					stress	0.85	21
						0.82	34
VA3	Min	475	190	256		0.79	54
						0.76	83
						0.73	124
						0.7	178
						0.67	247
VA4	Max	550	220	297		0.64	331
					High	0.61	429
						0.58	537
VA5	Max	475	190	256	mean	0.55	649
					stress	0.52	759
						0.49	856
VA6	Max	400	160	216		0.46	933
						0.43	983
						0.4	1000

[a]Scaled value (see Eq. (11))

test results. The block was repeated until final rupture. Rainflow analysis was used to evaluate VA loading in respect to CA load (Eq. (2)). Based on the fatigue test results in [7], the slope parameter $m = 3$ was used with rainflow method. The loading was constructed in a way that there were no cycles below constant amplitude fatigue limit (CAFL) and $m = 3$ could be used for each cycle. Fatigue performance when load block includes cycles below CAFL will be evaluated in future studies.

4 Fatigue test results and fractography

The CA fatigue test results from Ref. [7] were used as a baseline and they are illustrated as FAT curves with $m = 3$ slope parameter in Fig. 4. Datapoints for the reference specimens are given in [2, 7]. It can be seen that VA loading

with constant minimum and maximum loading resulted highly distinguishing results. The fatigue test results are presented with the nominal stress method and local stress method in Section 4. Further analysis is presented in Section 5 with multiparametric 4R method to consider mean stress correction.

The nominal stress method is shown as indicative results and comparison should be done only within similar specimens. Figure 4a and 4b illustrate fatigue test results for $d = 8$ mm and $d = 24$ mm specimens, respectively. The CA fatigue test results from [7] are shown as FAT curves with $m = 3$ slope parameter as a reference value to evaluate VA load's fatigue performance. The results suggest that fatigue tests where high mean stress was used have slightly decreased fatigue performance in comparison to the CA tests. Moreover, low mean stress test exceeds CA test fatigue life with a very significant margin. The
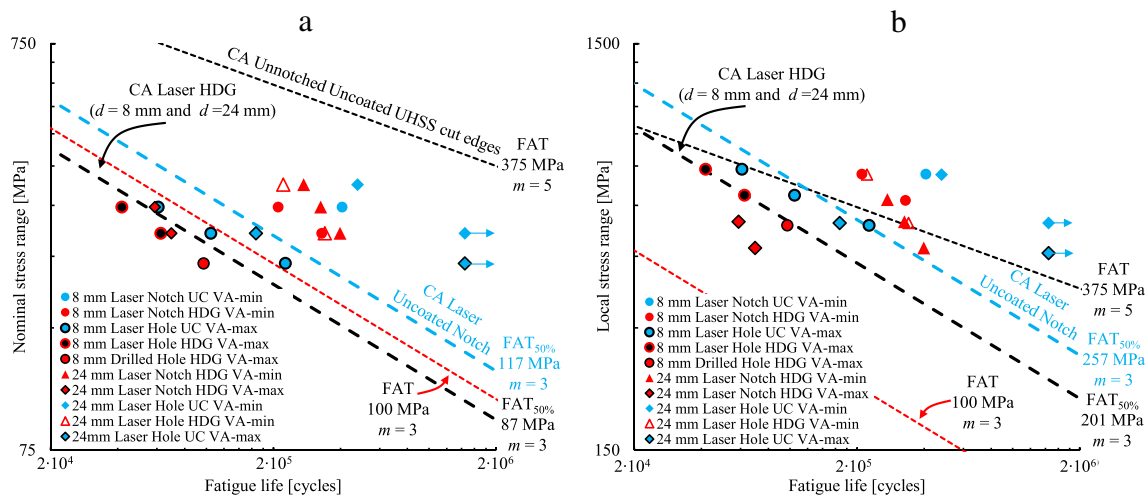

Fig. 4 (**a**) Nominal stress and (**b**) geometric SCF obtained stress fatigue test results. FAT values obtained from CA-loaded laser and mechanically cut ($d = 8$ & $d = 24$ mm combined)

difference in fatigue life between the examined low and high mean stress levels at the same stress range was around $N_{f,VA\ min\ load}/N_{f,VA\ max\ load} \approx 10$, which can be considered very major difference.

The local stress approach was found to reduce scatter when comparing the $d = 8$ mm and $d = 24$ mm specimens with internal (holes) and external notches. However, a major difference in test results between the constant minimum and maximum VA load raises question how to evaluate fatigue life even when only small scatter was found with similar loading type. When FAT values of both constant maximum and minimum are estimated separately, steep S–N curves ($m \approx 2$) are obtained with free slope when uncoated VA_{min} specimens are excluded.

Two uncoated laser cut specimens test were interrupted at the $1.4 \cdot 10^6$ cycles (200 blocks, see Appendix). A quasi-static tensile test was conducted after the interrupted fatigue test, and small (2–3 mm in length) cracks were found at the bottom of the notches. In S–N curve figures, this specimen is marked with an arrow (as a runout); even failure would have occurred at the higher number of cycles if test was continued.

The FAT values for uncoated and HDG specimens with division to constant minimum and maximum loads are given in Table 2. According to IIW and BS7608, the damage parameter $D = 0.5$ is used for VA load generally and $D = 0.2$, "for fluctuating mean stress" [9]. According to the fatigue test results, using $D = 0.2$ causes excessive safety factor as the results with high mean stress are close to the CA fatigue test results.

Fractography for similar specimens tested with CA load was presented in [7]. For this study, fractography was conducted to evaluate crack propagation with VA loading and differences in high and load mean stress specimens. Beach marks from block loading were easily detected from the specimens with the constant minimum loading whereas they were not visible in case of constant maximum load (Fig. 5a and 5b). The uncoated laser cut specimen crack initiated from region with highest surface roughness with influence from narrow brittle layer at the cut edge.

The VA load induced beach marks on fracture surfaces. The VA1 load with highest peak load was found to have the most significant marks for each block. A series of three SEM images was selected as an example for the crack propagation (Fig. 6). The fatigue life of the specimen was 66 blocks, and

20 blocks were calculated until 250-μm distance from cut surface was reached and counting become challenging due to small crack propagation rate. Most of the fatigue life is covered in short crack area and stress-based methods are effective in fatigue strength assessment. Use of linear-elastic fracture mechanics (LEFM) was demonstrated in [7] and it was found to be conservative. After HDG, the fatigue life measured in cycles reduces to 25–50% in respect to uncoated specimens [8]. The corresponding load was tested (Fig. 4) and fatigue life of 30 blocks was obtained which is reasonable considering initial crack length.

5 Parametric fatigue performance assessment

4R method application together with modelling initial cracks is based on fractography and obtaining local stresses with TCD method. Parameters given in Table 3 were used in analysis. $R_m = 1300$ MPa and $\sigma_{res} = 0$ MPa were used for all test series. Residual stresses on uncoated laser cut and drilled specimens could have been included on parametric model. However, defining residual stresses at HDG-induced crack tip is difficult. Laser cut uncoated specimens could be assessed with higher R_m value due to increase in hardness at HAZ. However, increased residual stresses would neglect the effect and excessive complexity of used model was targeted to avoid as the main emphasis of the paper is on VA load evaluation.

Point method (PM) was used, and critical distance (a) was varied to reduce the scatter. 4R method development aims to use true and measurable input parameters. Consequently, TCD method is needed to adjust stress level to match stresses with material curve. TCD method itself has only minor advantages on fatigue performance assessment in comparison to CA loads in [7] where it was successfully used to evaluate performance of specimens with different initial crack lengths with one FAT curve. With TCD method, the stress range is increased by including initial crack, but the majority of the increase takes place at compressive side which is not considered.

Notched specimens' ($d = 8$ mm) local cyclic behavior is illustrated in Fig. 7 including the effect of initial crack length and mean stress of the load block. After the 4R method mean stress correction, $\Delta\sigma_{k,ref}$ values of high

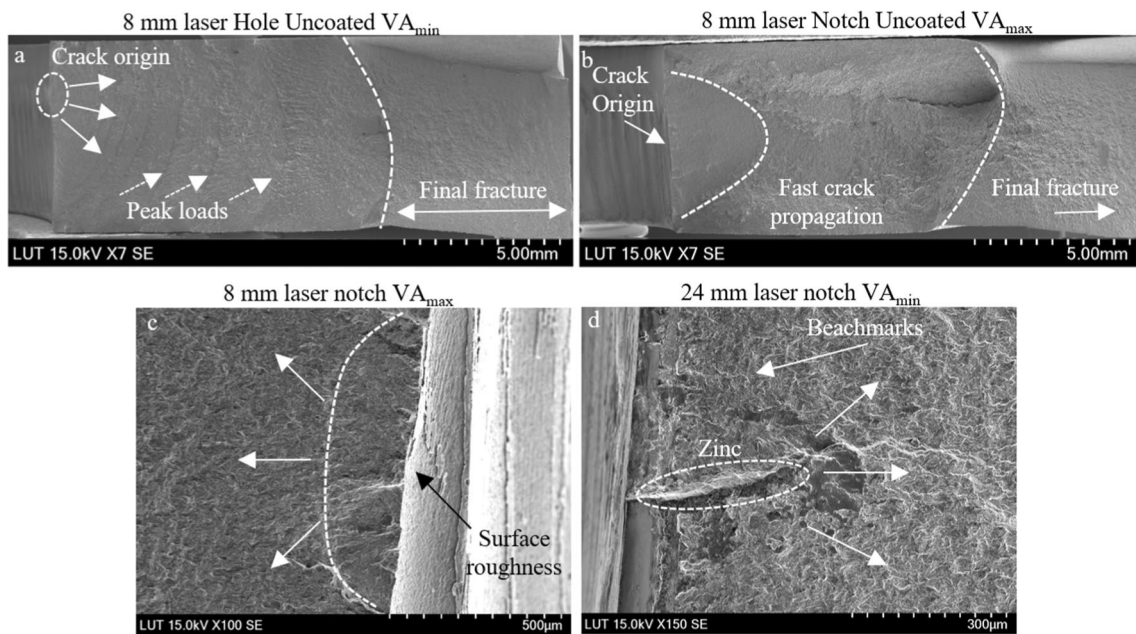| **Table 2** Fatigue performance	Specimen	Nominal stress FAT [MPa] and damage parameter [-] ($m=3$)				Local stress FAT [MPa] and damage parameter [-] ($m=3$)			
		HDG		Uncoated		HDG		Uncoated	
	VA_{min}	152	$D=5.33$	203	$D=5.22$	315	$D=3.85$	450	$D=5.37$
	VA_{max}	76	$D=0.67$	101	$D=0.64$	183	$D=0.75$	244	$D=0.82$

Fig. 5 Fractography showing (**a**) constant minimum laser cut hole, (**b**) constant maximum laser cut notch and details from (**c**) uncoated laser cut constant maximum and (**d**) laser cut HDG constant minimum specimens
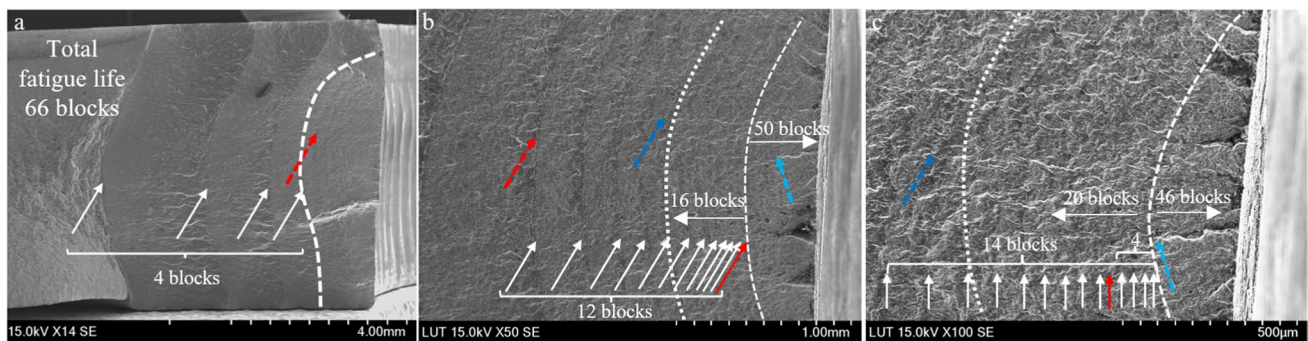

Fig. 6 Example of counting load blocks from VA1 load tested $d = 24$ mm laser cut hole

Table 3 Parameters used with 4R method

Specimen	Initial crack length [μm]		R_m [MPa]	σ_{res} [MPa]
	Uncoated	HDG	All	All
Laser notch	25	250	1300	0
Machined and drilled notches	10	125		

mean stress tested specimens increase in comparison to low mean stress ones. Four different cycles are highlighted with calculated R_{local} values shown in the figure. The smallest cycle is extreme example with variating local stress ratio R_{local} being -0.74 with constant minimum load

and 0.51 with constant maximum load in HDG specimens (stress level $\Delta\sigma_{21}$ in Fig. 7). The significantly shorter fatigue life of high mean stress specimens can be now explained with higher stress range on tensile side and R_{local} correction with Eq. (2) in case of 4R method. HDG with longer LME-based crack can be explained with higher stress range as shown with red color and low scatter can be found.

Finally, Fig. 8 presents the fatigue test results with the TCD-based 4R method in the reference coordinate system ($\Delta\sigma_{k,ref}$-N_f). A critical distance of $a = 0.1$ mm was found the most suitable with the applied VA loads, whereas $a = 0.04$ mm resulted in a lowest scatter when assessing the CA tests in [7]. Slightly scattered results with $a = 0.04$ mm critical distance are probably caused by residual stresses close to
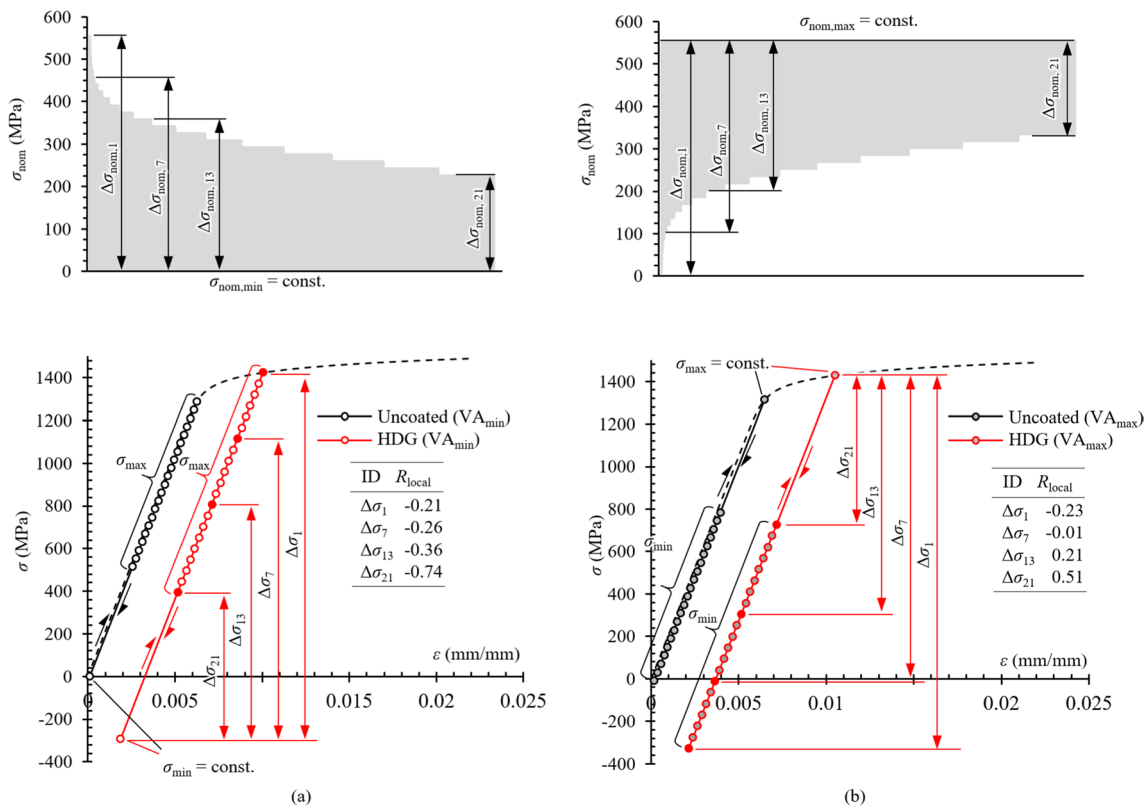
Fig. 7 R_{local} values for $d = 8$ mm uncoated (black) and HDG (red) with (**a**) constant minimum VA2 and (**b**) constant maximum VA4 loads

HDG-induced crack tip. Including tensile residual stresses in analysis, decrease in 4R reference stresses and scatter is visible in Fig. 8b. The uncoated laser cut notched specimen with VA6 (VA$_{max}$ with smallest $\Delta\sigma$) fatigue life matched to VA$_{min}$ loads. It can be seen that stress range $\Delta\sigma_{k,ref}$ varies as per the mean stress (VA$_{min}$ and VA$_{max}$ loads), and also considers existing pre-crack length enabling fatigue strength assessment with the master S–N curve approach.

A damage parameter $D = 1$ was found suitable for the fatigue tests conducted under variable amplitude

load—considering the VA data points, $D = 1.34$ (corresponding to a factor of 1.08 in fatigue strength with $m = 3.9$). The results had good agreement with the CA data for the same $a = 0.1$ mm critical distance applied in the analysis. It can be seen that scatter after using the 4R method has decreased to a low level ($T_\sigma = 1.25$ for the VA-loaded joints with $m = 3.9$) which is lower than with the CA data ($T_\sigma = 1.48$ for $a = 0.1$ mm, Ref. [7]). Similar master curve independently obtained from CA and VA tests increases the reliability of the introduced method.

Fig. 8 4R method fatigue test results with (**a**) 0.1-mm and (**b**) 0.04-mm critical distances in the mean stress–corrected reference stress system
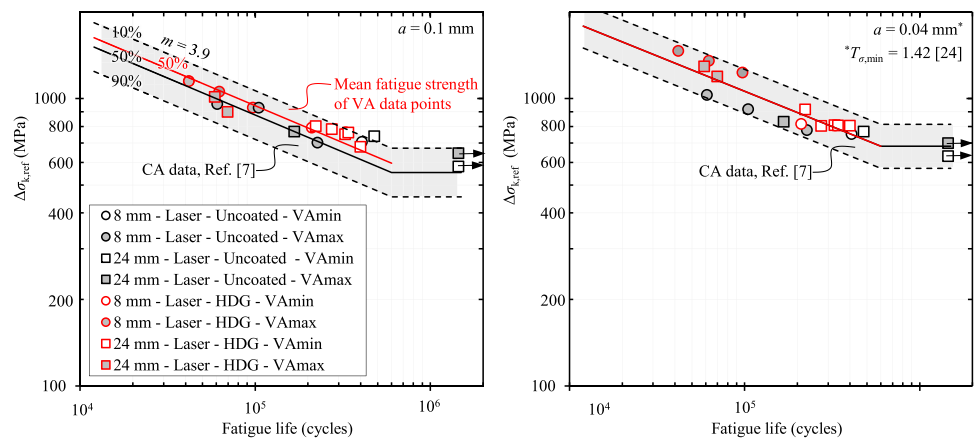
6 Discussion

Applications for the 4R method become highly valuable when assessing VA loads as it has an in-built approach to conduct mean stress correction. Interestingly, the high mean stresses ($R > 0$) have been found to have only minor influence on the fatigue performance under CA loads, as demonstrated, e.g., in [2, 8, 19] with CA-loaded laser cut and/or HDG specimens. The 4R method with the TCD approach has been applied in two studies for cut edges and is still currently under further development. In current study, similar blocks were continued until failure occurred. Varying frequency of high and low stress cycles in different mean stress levels could be still studied. However, the 4R method can be recommended to be applied, particularly, when assessing VA-loaded structures since it remains highly similar than with CA loads, whereas fatigue class-based method accuracy decreases at the same time that complexity increases with different damage parameters.

The parametric method will be further evaluated with shear cut specimen fatigue test with highly similar loading. Shear cutting results initial defect size in the middle of laser cutting and hot-dip galvanizing. However, high tensile residual stresses are induced in cutting process. Based on preliminary investigations, the results are in line with this study evaluated with local stress method. Evaluation with different steel grades provides insight on the master curve whether a single S–N (master) curve is sufficient, or fatigue capacity or applied critical distance should be corrected based on the material strength.

As a design recommendation for the geometric notches in VA loads (Table 4), a rainflow analysis together with a comparison to CA load design recommendation was found a good engineering practice with cut geometries. If this approach is used, the damage parameter is the most significant source of error. In this case, high (fluctuating) mean stress test resulted slightly lower performance than CA loads which still leads to relatively high D values, and $D = 0.5$ could be used on fatigue strength assessment with additional safety factor included. Without assessing local stress ratio, the additional fatigue life from low mean stress cases cannot be utilized.

Transparent and trustworthy input parameters for fatigue models are beneficial. When these parameters are documented, it enables further analysis based on literature.

On the other hand, well-documented procedure encourages including model in studies. Machine learning models are typically closed, and similar data is used in training and testing in many cases. To enable a use of the studied 4R method application, SEM fractography should be carefully conducted to avoid any misconceptions on the input parameters. Particularly, the presence of local imperfections is important due to their high influence on local SCFs. Material model can be extracted from the local hardness or by base material values if no major hardening or softening occurs due to the cutting process. The 4R method includes residual stress parameter; however, thus far, $\sigma_{res} = 0$ has been used as an input value since measuring the residual stresses in the vicinity of crack tip is difficult. Constant minimum loading was found to result smallest cycles below CAFL in as 4R corrected stresses. It is expected that these cycles are not effective to cause fatigue failure before fatigue crack size increases due to larger cycles. The effect of local behavior on partly compressive small cycles in respect to CAFL will be evaluated in future studies.

For the welded joints, a consideration on the effective notch stress (ENS) and TCD methods use should be evaluated. In welded structures, SCF varies according to the weld toe radius, transition angle, and weld shape, which can be modified, e.g., by means of the post-weld treatments (PWTs). Local imperfections with various sizes may exist if PWTs induce micro cracks to undercuts and cold laps. When assessing welded joints with sharp notches, the TCD method may be beneficial. Moreover, reasonable SCFs are highly important with 4R method for reasonable local behavior with selected material parameters.

7 Conclusions

Loading type (constant minimum or constant maximum) had a major influence on the fatigue life which highlights the importance of mean stress consideration in fatigue strength assessments. Conventionally, this has been considered through different damage sums for VA loads with different mean stress levels ($D = 0.2$ and $D = 0.5$). With the studied specimens, high mean stress load resulted in a slightly lower fatigue performance than CA loads

Table 4 Nominal and local stress method variable amplitude design recommendation

Notch category	Nominal FAT value $m = 3$		Local FAT value $m = 3$		Damage parameter D	
	Uncoated	HDG	Uncoated	HDG	High mean stress	Low mean stress
Laser cut	71	56	160	150	0.5	0.8
Machined and drilled	90	63	250	175		

$(D = 0.64; 0.75)$ whereas low mean stress specimens significantly exceeded CA load's fatigue performance $(D = 3.85; 5.33)$ when employing equivalent stresses.

The TCD-based 4R method application, considering local cyclic behavior, was found valid on fatigue strength assessment with the damage parameter $D = 1.0$. In particular, the 4R method was found to be well suitable for VA loads since the effect of local cyclic behavior is taken into account in assessments, and no major modifications to the method are needed in comparison to the 4R methodology for assessing CA loads. The introduced method will be further applied on welded joint fatigue performance assessment.

Appendix

Table 5 Fatigue test results

Specimen	Cycles [-]	Load ID	Note
24-mm laser notch HDG	273,520	VA1	
24-mm laser notch HDG	325,980	VA2	
24-mm laser notch HDG	398,420	VA3	
24-mm laser notch HDG	58,750	VA4	
24-mm laser notch HDG	69,570	VA5	
24-mm laser hole UC	478,100	VA1	
24-mm laser hole UC	1,448,800	VA3	Test interrupted Visible crack detected
24-mm laser hole UC	166,900	VA5	
24-mm laser hole UC	1,448,800	VA6	Test interrupted
24-mm laser hole HDG	221,360	VA1	
24-mm laser hole HDG	340,470	VA3	
8-mm laser notch UC	406,920	VA2	
8-mm laser notch HDG	210,090	VA2	
8-mm laser notch HDG	329,240	VA3	
8-mm laser hole HDG	41,760	VA5	
8-mm laser hole HDG	62,370	VA5	
8-mm laser hole UC	60,730	VA4	
8-mm laser hole UC	104,680	VA5	
8-mm laser hole UC	226,380	VA6	
8-mm drilled hole HDG	97,120	VA6	

UC uncoated, *HDG* hot-dip galvanized

Declarations

References

1. Wang T, Zhang H, Duan Y, et al (2022) Research on fatigue life prediction method of key component of turning mechanism based on improved TCD. Metals (Basel) 12:. https://doi.org/10.3390/met12030506
2. Lipiäinen K, Afkhami S, Ahola A, Björk T (2022) Evaluation of geometrical notch and quality effects in the fatigue strength assessment of ultra-high-strength steel cut edges. Structures 37:14. https://doi.org/10.1016/j.istruc.2022.01.069
3. Taylor D (2008) The theory of critical distances. Eng Fract Mech. https://doi.org/10.1016/j.engfracmech.2007.04.007
4. Souto CDS, Gomes VMG, Figueiredo M et al (2021) Fatigue behaviour of thin-walled cold roll-formed steel sections. Int J Fatigue 149:106299. https://doi.org/10.1016/j.ijfatigue.2021.106299
5. Ahola A, Lipiäinen K, Afkhami S et al (2022) Fatigue performance of the welded details of an old, demolished steel railway bridge. Eng Struct 256:113966. https://doi.org/10.1016/j.engstruct.2022.113966
6. Braun M, Ahola A, Milaković AS, Ehlers S (2022) Comparison of local fatigue assessment methods for high-quality butt-welded joints made of high-strength steel. Forces Mech 6. https://doi.org/10.1016/j.finmec.2021.100056
7. Lipiäinen K, Ahola A, Kaijalainen A, Björk T (2022) Fatigue performance of notched and hot-dip galvanized laser and mechanically cut S960 steel components considering local defects with the theory of critical distances. Int J Fatigue. https://doi.org/10.1016/j.ijfatigue.2022.107127
8. Lipiäinen K, Ahola A, Virolainen E et al (2022) Fatigue strength of hot-dip galvanized S960 cut edges and longitudinal welds. J Constr Steel Res 189:107083. https://doi.org/10.1016/j.jcsr.2021.107083
9. Hobbacher AF (2016) Recommendations for fatigue design of welded joints and components. Springer

10. BSI Standards Publication (2015) BS 7608 - guide to fatigue design and assessment of steel products
11. Schijve J (2009) Fatigue of structures and materials. Springer, Netherlands, Dordrecht
12. Shams-Hakimi P, Al-Karawi H, Al-Emrani M (2022) High-cycle variable amplitude fatigue experiments and design framework for bridge welds with high-frequency mechanical impact treatment. Steel Constr 15. https://doi.org/10.1002/stco.202200003
13. Leitner M, Stoschka M, Barsoum Z, Farajian M (2020) Validation of the fatigue strength assessment of HFMI-treated steel joints under variable amplitude loading. Weld World 64:1681–1689. https://doi.org/10.1007/s40194-020-00946-8
14. Liu X, Zhang Y-H, Wang B, Sun X (2022) Influence of the mean stress on the fatigue life of welded joints under variable amplitude loading. Int J Fatigue 163:106972. https://doi.org/10.1016/j.ijfatigue.2022.106972
15. Bibbo ND, Larsen ML, Baumgartner J, Arora V (2022) An improved rainflow counting method for multiaxial stress states using the minimum circumscribed circle method to identify shear stress ranges. Int J Fatigue 163:106997. https://doi.org/10.1016/j.ijfatigue.2022.106997
16. Nykänen T, Mettänen H, Björk T, Ahola A (2017) Fatigue assessment of welded joints under variable amplitude loading using a novel notch stress approach. Int J Fatigue 101:177–191. https://doi.org/10.1016/j.ijfatigue.2016.12.031
17. Ahola A, Skriko T, Björk T (2020) Fatigue strength assessment of ultra-high-strength steel fillet weld joints using 4R method. J Constr Steel Res 167. https://doi.org/10.1016/j.jcsr.2019.105861
18. Köhler M, Jenne S, Pötter K, Zenner H (2017) Load assumption for fatigue design of structures and components: counting methods, safety aspects, practical application. Springer. https://doi.org/10.1007/978-3-642-55248-9
19. Lipiäinen K, Ahola A, Skriko T, Björk T (2020) Fatigue strength characterization of high and ultra-high-strength steel cut edges. Eng Struct. https://doi.org/10.1016/j.engstruct.2020.111544